J Appl Electrochem (2013) 43:9–13
DOI 10.1007/s10800-012-0498-x

SHORT COMMUNICATION

Electrochemical growth of self-organized TiO_2–WO_3 composite nanotube layers: effects of applied voltage and time

Yoon-Chae Nah · Nabeen K. Shrestha · Doohun Kim · Patrik Schmuki

Received: 14 August 2012 / Accepted: 29 October 2012 / Published online: 7 November 2012

Abstract The present work demonstrates that morphology of TiO_2–WO_3 composite nanotubes formed by alloy anodization can be tuned by controlling applied voltages and time. Distinctive tube morphology can be formed by applying a voltage of more than 80 V. Nanotube diameter and length have a linear relationship with the anodization voltage with a current efficiency of almost 100 %. Furthermore, compared to pure TiO_2, the composite nanotubes show a very uniform tube diameter along the tube axis even at the extended anodization time.

Keywords Ti–W alloy · Anodization · Self-organized · Composite nanotubes

1 Introduction

In the past decades, TiO_2 nanotubes have received great interest due to their potential abilities to apply for biomedical applications [1–3], photovoltaic cells [4, 5], photocatalysts [6, 7], and electrochromic devices [8–10]. TiO_2 nanotubes could be prepared using various physical or chemical methods. One of the prominent approaches to prepare TiO_2 nanostructures is electrochemical anodization. Self-organized TiO_2 nanotubes based on an electrochemical anodization process have been widely studied because they can provide a vertically aligned structure to the electrode with high surface area, which is optimal especially for the electrochemical or electronic applications as the nanotubes directly grow on the Ti-metal surface which can be used directly as a back contact electrode. More importantly, the tube length and diameter can be controlled by tailoring the electrochemical conditions such as the applied potential, anodization time, and the pH of electrolyte [11].

In addition to TiO_2, the fabrication of self-organized nanostructure has been investigated under optimized anodization conditions in fluoride-containing electrolytes for various valve metals such as Zr [12], Hf [13], Nb [14], Ta [15], W [16], and V [17]. Self-organized nanotube formation was also studied for several alloys with two components [18–21] and multicomponents [22–25]. For composite oxide nanotubes, bimodal or inhomogeneous tube morphology can be observed due to the preferential dissolution [24, 25].

Several efforts have been made to employ a mixed TiO_2–WO_3 system in order to enhance the photocatalytic [26], photoelectrochemical [27], and electrochromic efficiency [28]. Fabrication of the nanotubular structure may lead to new functionalities of TiO_2–WO_3 composites such as electrochromic electrodes, and a control of morphology and composition of the nanoarchitectures is significantly important for their electronic properties. In our preliminary studies, we demonstrated the formation of highly ordered and self-organized TiO_2–WO_3 composite nanotubes by the TiW alloy anodization in organic electrolyte with HF [29]. In the present work, we investigate the feasibility to control the morphology of TiO_2–WO_3 nanotubes by controlling the anodization parameters such as applied voltages and time.

Y.-C. Nah
School of Energy, Materials and Chemical Engineering, Korea University of Technology and Education, Cheonan 330-708, Republic of Korea

Y.-C. Nah · N. K. Shrestha · D. Kim · P. Schmuki (✉)
Department of Materials Science, WW4-LKO, University of Erlangen-Nuremberg, Martensstr. 7, 91058 Erlangen, Germany
e-mail: schmuki@ww.uni-erlangen.de

2 Experimental

TiW alloy plates (Ti:W = 91:9 at.%, GKSS Forschungszentrum in Geesthacht, Germany) were used as the substrate. The plates were first pretreated by polishing with silicon carbide abrasive paper, 6 μm diamond abrasives, and colloidal silica successively. For comparison, Ti sheets (0.1 mm, 99.6 %, Advent Research Materials) were used as the substrates for growth of TiO_2 nanotubes after the polishing treatment. Before use, all samples were sonicated in acetone, isopropanol, and methanol successively, followed by rinsing with deionized (DI) water and drying in a nitrogen stream.

To obtain nanotube layers, Ti and TiW alloy samples were anodized in a solution of ethylene glycol (EG, Riedel-de Haën) containing 0.2 M HF (40 vol%, Merck). Before using, the electrolyte was aged by anodizing a Ti foil at 120 V for 24 h. This sort of electrolyte aging is performed in order to improve the conductivity of the electrolyte and generate dissolved Ti complexes, which assists to minimize the solution ohmic drop and equilibrates the solution with reaction products—it not only thus reduces the chemical dissolution rate during anodization, but also increases the growth rate of the nanotubes [30]. In order to investigate the influence of voltage and anodization time on tube morphology, voltages in the range of 60 to 140 V were applied for a given time and then at each voltage, anodization was carried out for the desired length of time. A field-emission scanning electron microscope (Hitachi FE-SEM S4800) was used to investigate morphological characteristics of the samples. The thickness and diameter of the nanotubes were determined from cross-section images.

3 Results and discussion

Figure 1 shows SEM images of the nanotube layers formed on the TiW alloy surface at 100 V in the EG electrolyte containing 0.2 M HF. The bottom and the cross-section images were obtained from mechanical cracking of the sample. Obviously, a highly ordered layer is produced that consists of a porous layer on the top (Fig. 1b) and closed tube on the bottom (Fig. 1d). A top oxide layer has formed with worm-like small pores underneath that just show a transition to a self-organized nanotube layer. The diameter of the small pores on the top layer is about 50 nm and the thickness of the porous layers is about 250 nm. The thickness of the top porous layer can be decreased by chemical dissolution as the anodization time is prolonged [31]. The tube wall in Fig. 1c shows that the tube wall surface is not very smooth, but it has a ripple structure, which is usually caused by the presence of even a small amount of water in the electrolyte [32]. Overall, the tubes have a length of about 3.8 μm for 1 h of anodization and have a diameter of ca. 190 nm. Almost the same outer

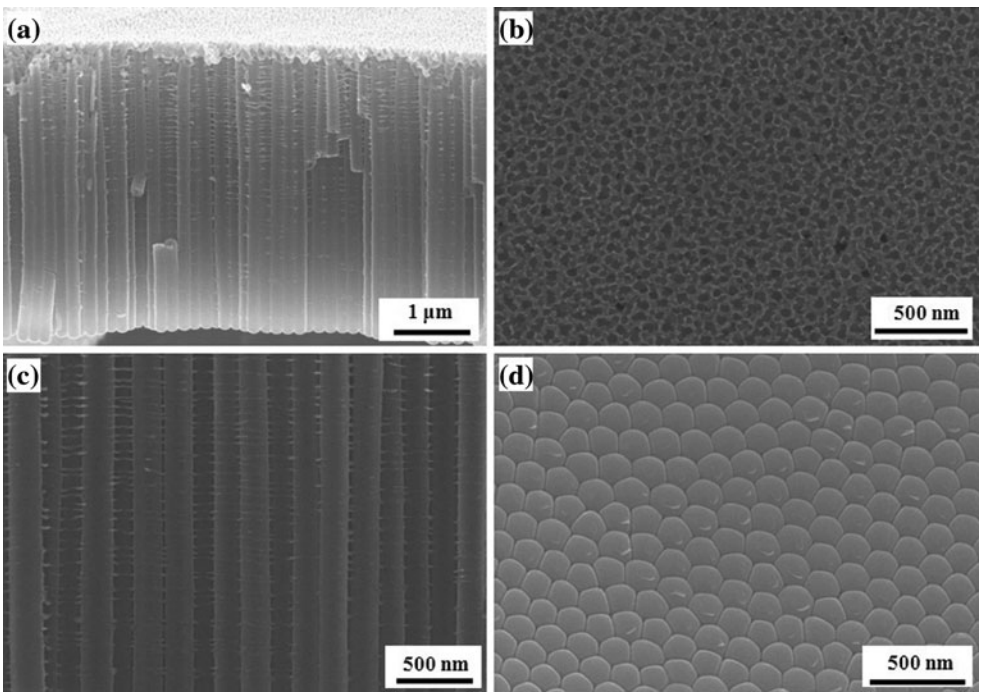

Fig. 1 SEM images of ordered oxide nanotube layers grown on Ti9W alloy by anodization in a solution of ethylene glycol with 0.2 M HF at 100 V for 1 h; **a**, **c** *cross-sectional view*, **b** *top view*, and **d** *bottom view*

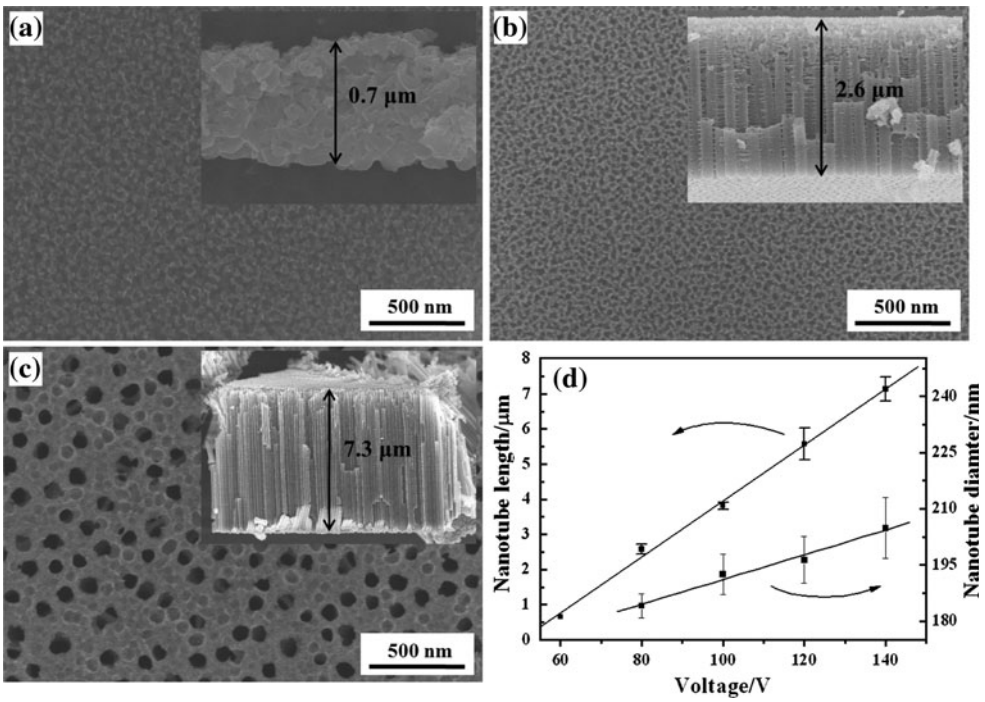

Fig. 2 SEM images of TiO_2–WO_3 nanotube layers anodized at different voltages: **a** 60, **b** 80, and **c** 120 V. The *insets* show the cross-sectional images of each layer. **d** Dependence of the length and diameter of TiO_2 and TiO_2–WO_3 nanotubes on the anodization

diameter along the tube axis is observed, which shows a very uniform and straight morphology.

In order to study the influence of the anodization potential, the tube morphology was investigated at various anodization potentials. Figure 2a–c shows the surface and cross-section images of TiO_2–WO_3 nanotubes grown at different anodization potential. When anodization was performed at 60 V for 1 h, no clear tubular or distinct pore structure was obtained. The resulting pore structure consisted of small pores that were interconnected to each other rather than a pore having a single cannel behavior. However, increasing the applied voltage to 80 V, a well-developed nanotube structure with a diameter of ca. 190 nm and a length of ca. 2.6 μm was obtained. On the top of this tubular structure, a porous initiation layer with a pore size of ca. 30 nm was obtained. A further increase in the voltage to 140 V led to the formation of a longer nanotube layer with a diameter of ca. 205 nm and length of 7.3 μm. The initiation pore size at this voltage enlarged to ca. 80 nm. As in the case of TiO_2 and other TiO_2-based composite nanotubes [11, 20, 25], a linear relationship among tube diameter, tube length, and anodization potential is observed also for TiO_2–WO_3 nanotubes (Fig. 2d). The linear behavior between the voltage and the tube length is ascribed to the fact that the thickness of anodic oxide film increases linearly with the potential of the formation of a compact oxide.

Valuable information can be obtained by investigating the relationship between electrical charge passed during the anodization and the resulting tube length. Figure 3 shows the thickness of nanotube layers at different anodization voltages with respect to the total charge density recorded during the anodization process. The dashed line is obtained by the theoretic calculation based on the Faraday's law, assuming the electrochemical anodization to be a ten-electron reaction (four for TiO_2 and six for WO_3) with 100 % current efficiency and the volume expansion from the alloy to the oxide is the vertical direction (one-dimensional) against the substrate [33, 34]. The theoretic relationship can be express as below:

$$L = \frac{Q}{10F} \times \left\{ \frac{M(\mathrm{TiO_2})}{\rho(\mathrm{TiO_2})} + \frac{M(\mathrm{WO_3})}{\rho(\mathrm{WO_3})} \right\}$$

where M(TiO_2) and M (WO_3) are the molar masses of TiO_2 and WO_3, the values of which are 79.88 and 231.84 g mol^{-1}, respectively. $\rho(TiO_2)$ and $\rho(WO_3)$ are the densities of TiO_2 and WO_3, the values of which are 3.89 [35] and 7.16 g cm^{-3} [36], respectively. Q is the total charge density measured during the anodization process and F is the Faraday constant. In Figure 3, the measured length is well matched with the calculated value, which means that the composite TiO_2–WO_3 nanotube can be grown with the current efficiency of almost 100 %. However, in case of 60 V, the efficiency is significantly less, which is possibly due to the ill-defined and non-vertical formation of oxide nanotube layers.

Apart from the anodization voltage, another factor to manipulate the nanotube length is the anodization time. Figure 4a shows that the nanotube length has a linear relationship with the anodization time up to about 120 min; after that, the growth rate gradually decreases. This effect can be due to chemical dissolution of the layer at the top [37].

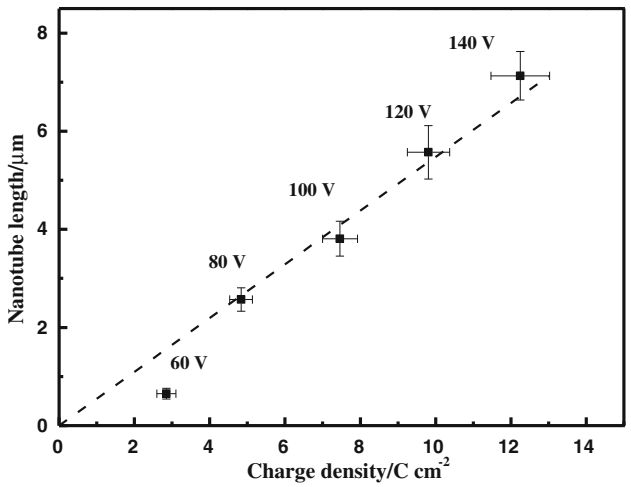

Fig. 3 Dependence of nanotube length on charge density. The *dashed line* shows the theoretic values calculated from Faraday's law assuming a 100 % current efficiency

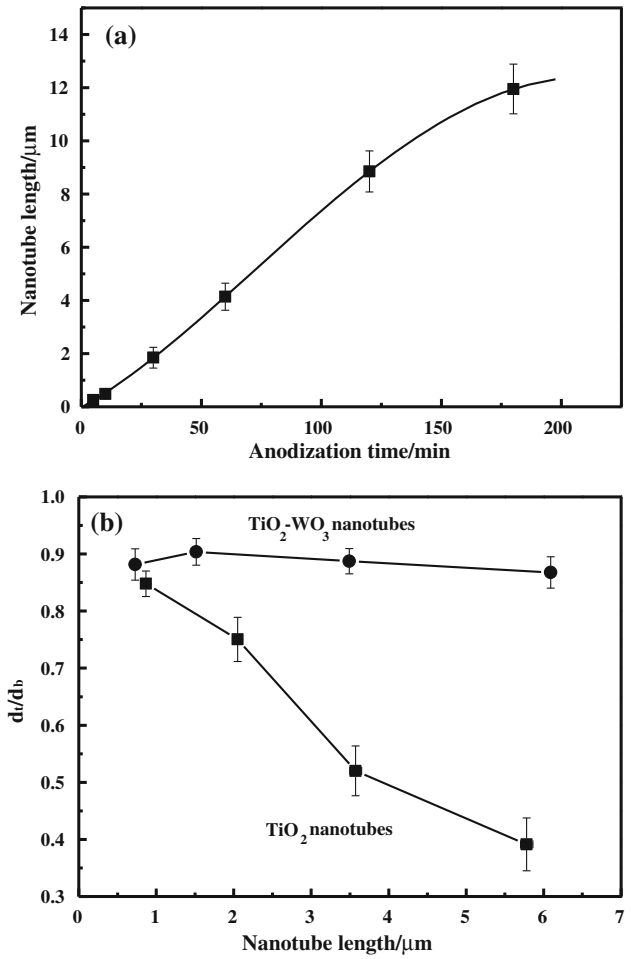

Fig. 4 **a** Nanotube length as a function of anodization time and **b** dependence of ratio between d_t and d_b on length of TiO_2 and TiO_2–WO_3 nanotubes. The d_t and d_b indicate diameter near tube *top* and near tube *bottom*, respectively

Fluoride ions in the electrolyte dissolve the oxide layer with the time leading to the etching of the tube tops. When anodization time is sufficiently prolonged, the relationship will be leveled off where electrochemical formation of nanotubes is stabilized by the chemical dissolution.

A more interesting characteristic for the morphology of mixed oxide nanotubes is that the tube is very straight aligned, meaning the diameter is uniform along the tube length. Figure 4b shows the ratio between tube diameter near the bottom (d_b) and the top (d_t) of TiO_2 and TiO_2–WO_3 nanotube layers as a function of tube length which is controlled by anodization time. For shorter tubes, both TiO_2 and TiO_2–WO_3 have a uniform tube diameter along the length where the ratio is about 0.9. For composite oxide nanotubes, this straight tube morphology is also shown in the longer tube (>6 μm) obtained by an extended anodization time, while in case of TiO_2 nanotubes, the ratio gradually decreases with the tube length and finally is <0.4 for longer tubes. Considering that the dissolution of the tube has preferentially occurred at the tube top, the decrease in the ratio is attributed to the thinning of the tube wall. In other words, compared to TiO_2 nanotubes, TiO_2–WO_3 nanotubes show the enhanced resistance against chemical dissolution, leading to a very straight alignment of the tube morphology.

4 Conclusions

In summary, the morphology of TiO_2–WO_3 composite nanotubes formed by anodization of TiW alloy can be controlled in a wide range of applied voltages and time. Distinctive nanotube morphology can be formed by applying a moderate voltage greater than 60 V. Nanotube diameter and length have a linear relationship with the anodization voltage with a current efficiency of almost 100 %. Furthermore, compared to pure TiO_2, the composite nanotubes show a very straight morphology even at the extended anodization time.

Acknowledgments This work was supported by DFG and FP-6 [Ti-nanotubes]. Dr. M. Oehring at the GKSS Forschungszentrum in Geesthacht is also acknowledged for providing the Ti–W alloys. Y. C. Nah was supported by the Basic Science Research Program through the National Research Foundation of Korea (NRF) funded by the Ministry of Education, Science and Technology (2012R1A1A1014075). N.·K. Shrestha was supported by the Alexander von Humboldt Foundation.

References

1. Tsuchiya H, Macak JM, Muller L, Kunze J, Muller F, Greil P, Virtanen S, Schmuki P (2006) Hydroxyapatite growth on anodic TiO_2 nanotubes. J Biomed Mater Res Part A 77A:534–541. doi:10.1002/jbm.a.30677
2. Park J, Bauer S, von der Mark K, Schumki P (2007) Nanosize and vitality: TiO_2 nanotube diameter directs cell fate. Nano Lett 7:1686–1691. doi:10.1021/nl070678d

3. Shrestha NK, Macak JM, Schmidt-Stein F, Hahn R, Mierke CT, Fabry B, Schmuki P (2009) Magnetically guided titania nanotubes for site-selective photocatalysis and drug release. Angew Chem Int Ed 48:969–972. doi:10.1002/anie.200804429
4. Kongkanand A, Tvrdy K, Takechi K, Kuno M, Kamat PV (2008) Quantum dot solar cells. Tuning photoresponse through size and shape control of CdSe–TiO_2 architecture. J Am Chem Soc 130:4007–4015. doi:10.1021/ja0782706
5. Adachi M, Murata Y, Okada I, Yoshikawa S (2003) Formation of titania nanotubes and applications for dye-sensitized solar cells. J Electrochem Soc 150:G488–G493. doi:10.1149/1.1589763
6. Albu SP, Ghicov A, Macak JM, Hahn R, Schmuki P (2007) Self-organized, free-standing TiO_2 nanotube membrane for flow-through photocatalytic applications. Nano Lett 7:1286–1289. doi:10.1021/nl070264k
7. Macak JM, Zlamal M, Krysa J, Schmuki P (2007) Self-organized TiO_2 nanotube layers as highly efficient photocatalysts. Small 3:300–304. doi:10.1002/smll.200600426
8. Hahn R, Ghicov A, Tsuchiya H, Macak JM, Muñoz AG, Schmuki P (2007) Lithium-ion insertion in anodic TiO_2 nanotubes resulting in high electrochromic contrast. Phys Status Solidi A Appl Mater 204:1281–1285. doi:10.1002/pssa.200674310
9. Ghicov A, Tsuchiya H, Hahn R, Macak JM, Muñoz AG, Schmuki P (2007) TiO_2 nanotubes: H^+ insertion and strong electrochromic effects. Electrochem Commun 8:528–532. doi:10.1016/j.elecom.2006.01.015
10. Ghicov A, Albu SP, Macak JM, Schmuki P (2008) High-contrast electrochromic switching using transparent lift-off layers of self-organized TiO_2 nanotubes. Small 4:1063–1066. doi:10.1002/smll.200701244
11. Macak JM, Tsuchiya H, Ghicov A, Yasuda K, Hahn R, Bauer S, Schmuki P (2007) TiO_2 nanotubes: self-organized electrochemical formation, properties and applications. Curr Opin Solid State Mater Sci 11:3–18. doi:10.1016/j.cossms.2007.08.004
12. Tsuchiya H, Macak JM, Taveira LV, Schmuki P (2005) Fabrication and characterization of smooth high aspect ratio zirconia nanotubes. Chem Phys Lett 410:188–191. doi:10.1016/j.cplett.2005.05.065
13. Tsuchiya H, Schmuki P (2005) Self-organized high aspect ratio porous hafnium oxide prepared by electrochemical anodization. Electrochem Commun 7:49–52. doi:org/10.1016/j.elecom.2004.11.004
14. Sieber I, Hildebrand H, Friedrich A, Schmuki P (2005) Formation of self-organized niobium porous oxide on niobium. Electrochem Commun 7:97–100. doi:org/10.1016/j.elecom.2004.11.012
15. Sieber I, Kannan B, Schmuki P (2005) Self assembled porous tantalum oxide prepared in H_2SO_4/HF electrolyte. Electrochem Solid-State Lett 8:J10–J12. doi:10.1149/1.1859676
16. Tsuchiya H, Macak JM, Sieber I, Taveira L, Ghicov A, Sirotna K, Schmuki P (2005) Self-organized porous WO_3 formed in NaF electrolytes. Electrochem Commun 7:295–298. doi:10.1016/j.elecom.2005.01.003
17. Yang Y, Albu SP, Kim D, Schmuki P (2011) Enabling the anodic growth of highly ordered V_2O_5 nanoporous/nanotubular structures. Angewandte Chem Int Ed 50:9071–9075. doi:10.1002/anie.201104029
18. Berger S, Tsuchiya H, Schmuki P (2008) Transition from nanopores to nanotubes: self-ordered anodic oxide structures on titanium–aluminides. Chem Mater 20:3245–3247. doi:10.1021/cm8004024
19. Yasuda K, Schmuki P (2007) Formation of self-organized zirconium titanate nanotube layers by alloy anodization. Adv Mater 19:1757–1760. doi:10.1002/adma.200601912
20. Shrestha NK, Nah Y-C, Tsuchiya H, Schmuki P (2009) Self-organized nano-tubes of TiO_2–MoO_3 with enhanced electrochromic properties. Chem Commun 15:2008–2010. doi:10.1039/B820953G
21. Yang Y, Kim D, Yang M, Schmuki P (2011) Vertically aligned mixed V_2O_5–TiO_2 nanotube arrays for supercapacitor applications. Chem Commun 47:7746–7748. doi:10.1039/C1CC11811K
22. Macak JM, Tsuchiya H, Taveira L, Ghicov A, Schmuki P (2005) Self-organized nanotubular oxide layers on Ti-6Al–7Nb and Ti–6Al–4 V formed by anodization in NH_4F solutions. J Biomed Mater Res 75 A:928–933. doi:10.1002/jbm.a.30501
23. Tsuchiya H, Macak JM, Ghicov A, Tang YC, Fujimoto S, Niinomi M, Noda T, Schmuki P (2006) Nanotube oxide coating on Ti–29Nb–13Ta–4.6Zr alloy prepared by self-organizing anodization. Electrochim Acta 52:94–101. doi:10.1016/j.electacta.2006.03.087
24. Tsuchiya H, Macak JM, Ghicov A, Schmuki P (2006) Self-organization of anodic nanotubes on two size scales. Small 2:888–891. doi:10.1002/smll.200600035
25. Feng X, Macak JM, Schmuki P (2007) Flexible self-organization of two size-scales oxide nanotubes on Ti45Nb alloy. Electrochem Commun 9:2403–2407. doi:10.1016/j.elecom.2007.07.007
26. Keller V, Bernhardt P, Garin F (2003) Photocatalytic oxidation of butyl acetate in vapor phase on TiO_2, Pt/TiO_2 and WO_3/TiO_2 catalysts. J Catal 215:129–138. doi:10.1016/S0021-9517(03)00002-2
27. De Tacconi NR, Chenthamarakshan CR, Rajeshwar K, Pauporté T, Lincot D (2003) Pulsed electrodeposition of WO_3–TiO_2 composite films. Electrochem Commun 5:220–224. doi:10.1016/S1388-2481(03)00021-3
28. De Tacconi NR, Chenthamarakshan CR, Wouters KL, MacDonnell FM, Rajeshwar K (2004) Composite WO_3–TiO_2 films prepared by pulsed electrodeposition: morphological aspects and electrochromic behavior. J Electroanal Chem 566:249–256. doi:10.1016/j.jelechem.2003.11.033
29. Nah Y-C, Ghicov A, Kim D, Berger S, Schmuki P (2008) TiO_2–WO_3 composite nanotubes by alloy anodization: growth and enhanced electrochromic properties. J Am Chem Soc 130:16154–16155. doi:10.1021/ja807106y
30. Lee K, Kim J, Kim H, Lee Y, Tak Y, Kim D, Schmuki P (2009) Effect of electrolyte conductivity on the formation of a nanotubular TiO_2 photoanode for a dye-sensitized solar cell. J Korean Phys Soc 54:1027–1031. doi:10.3938/jkps.54.1027
31. Feng X, Macak JM, Schmuki P (2007) Robust self-organization of oxide nanotubes over a wide pH range. Chem Mater 19:1534–1536. doi:10.1021/cm063042g
32. Valota A, LeClere DJ, Skeldon P, Curioni M, Hashimoto T, Berger S, Kunze J, Schmuki P, Thompson GE (2009) Influence of water content on nanotubular anodic titania formed in fluoride/glycerol electrolytes. Electrochim Acta 54:4321–4327. doi:10.1016/j.electacta.2009.02.098
33. Yasuda K, Schmuki P (2007) Control of morphology and composition of self-organized zirconium titanate nanotubes formed in $(NH_4)_2SO_4$/NH_4F electrolytes. Electrochim Acta 52:4053–4061. doi:10.1016/j.electacta.2006.11.023
34. Berger S, Macak JM, Kunze J, Schmuki P (2008) High-efficiency conversion of sputtered Ti thin films into TiO_2 nanotubular layers. Electrochem Solid-State Lett 11:C37–C40. doi:10.1149/1.2908199
35. Pringle JPS (1979) The anodic oxidation of superimposed metallic layers: theory. Electrochim Acta 25:14231437. doi:10.1016/0013-4686(80)87157-X
36. Hoang-Van C, Zegaoui O (1995) Appl Catal A Gen 130:89–103. doi:org/10.1016/0926-860X(95)00096-8
37. Yasuda K, Schmuki P (2007) Formation of self-organized zirconium titanate nanotube layers by alloy anodization. Adv Mater 19:1757–1760. doi:10.1002/adma.200601912